Journal of Petroleum Science and Engineering 157 (2017) 990–998

Contents lists available at ScienceDirect

Journal of Petroleum Science and Engineering

journal homepage: www.elsevier.com/locate/petrol

Operator-based linearization for general purpose reservoir simulation

Mark Khait, Denis V. Voskov *

Delft University of Technology, Delft, The Netherlands

ARTICLE INFO

Keywords:
Nonlinear solvers
Physics coarsening
Operator-based linearization

ABSTRACT

General purpose reservoir simulation is based on the solution of governing equations describing mass and energy transfer in the subsurface. The solution process requires the linearization of strongly nonlinear governing equations. Usually, a Newton-based method is used for the linearization. This method demands the assembly of Jacobian and residual for a fully coupled system of equations. Recently, a new linearization approach was proposed and tested for binary systems. The key idea of the Operator Based Linearization (OBL) approach is to transform the discretized mass and energy conservation equations to an operator form which separates space-dependent and state-dependent properties of governing equations. This transformation provides the opportunity to approximate the representation of exact physics (physical properties) of a problem. Specifically, each term of the conservation equations is presented as the product of two different operators. The first operator depends on the current physical state of a system and contains fluid properties, such as density, viscosity, relative permeability, etc. The second operator captures both spatially altered properties, such as permeability, and the rest of state variables, such as pressure in the discrete approximation of gradient. All state-dependent operators are uniformly parametrized within the physical space of the problem (pressure-composition intervals). During simulation process, a multilinear interpolation is applied to approximate the first type of operators, while the second type of operators is processed based on conventional approach. In this work, we extended the approach to thermal systems with an arbitrary number of components. Besides, we significantly improved the performance of OBL employing adaptive parametrization technique. We tested the approach for truly multi-component thermal systems of practical interest. The computational performance, accuracy, and robustness of a new method were demonstrated against the conventional approach.

1. Introduction

Numerical simulations are essential for the modern development of subsurface reservoirs (Aziz and Settari, 1979). They are widely used for the evaluation of oil recovery efficiency, performance analysis, and various optimization problems. Due to the complexity of underlying physical processes and considerable uncertainties in the geological structure of reservoirs, there is a persistent demand for accurate and efficient models. In order to increase the accuracy of a model, one can apply a finer computational grid in space or time, or use a more detailed description of the fluids such as in thermal-compositional model. However, the improvement in the accuracy of models is usually counterbalanced by the reduction in the turnaround time of simulation. In the presence of ensemble optimization or stochastic solution based on a version of Monte Carlo approach, demanding thousands of simulations, the performance of forward simulation becomes a primary issue (Muller et al., 2016).

Space and time approximations usually introduce nonlinearity to the system of governing equations, further enhanced by complex behavior of multiphase fluid flow. Numerical solution of such systems with millions of unknowns is the only known way to complete simulation in feasible time. The particular set of independent variables (i.e., nonlinear unknowns) is defined by the nonlinear formulation of the actual simulation framework (Cao, 2002). During linearization stage, all properties and their derivatives need to be determined with respect to nonlinear unknowns. The linearization of the nonlinear system requires Jacobian assembly and consumes a significant portion of simulation time, especially for complex physical processes (Zaydullin et al., 2016).

Several conventional linearization approaches exist, though neither of them is robust, flexible, and computationally efficient all at once. Numerical derivatives provide flexibility in the nonlinear formulation (see Xu et al., 2011 for example), but a simulation based on numerical derivatives may lack robustness and performance (Vanden and

* Corresponding author. Faculty of Civil Engineering and Geosciences, Delft University of Technology, Stevinweg 1, Delft, 2628 CN, The Netherlands.
E-mail address: D.V.Voskov@tudelft.nl (D.V. Voskov).

http://dx.doi.org/10.1016/j.petrol.2017.08.009
Received 23 November 2016; Received in revised form 27 July 2017; Accepted 2 August 2017
Available online 5 August 2017

Orkwis, 1996). Straightforward hand-differentiation is the workhorse strategy in modern commercial simulators (Schlumberger, 2007; Cao et al., 2009). However, this approach requires introduction of a complicated framework for storing and evaluating derivatives for each physical property, which in turn reduces the flexibility of a simulator to incorporate new physical models and increases probability for potential errors. The development of Automatic Differentiation (AD) technique allows preserving both flexibility and robustness in derivative computations. In reservoir simulation, the AD-based library (ADETL) was introduced by Younis (2011). Using the capabilities of ADETL, the Automatic Differentiation General Purpose Research Simulator (ADGPRS) was developed (Voskov and Tchelepi, 2012; Zhou et al., 2011). Later, the AD technique becomes more demanded in research frameworks for reservoir simulation (Krogstad et al., 2015). Being attractive from the perspective of flexibility, the AD technique by design inherits computational overhead, which affects the performance of reservoir simulation (Khait and Voskov, 2017).

A novel linearization approach called Operator-Based Linearization (OBL), where performance, robustness, and flexibility can be combined without compromise, was introduced in Voskov (2017). Each term in discretized conservation equations is represented by the product of two operators: state- and space-dependent. The state-dependent operators are adaptively parametrized over the physical space of a simulation problem, while space-dependent operators are applied in the conventional manner. During the course of the simulation, the state-dependent operators are calculated based on the multilinear interpolation in multidimensional space of nonlinear parameters. The performance gain of Jacobian assembly with OBL reaches an order of magnitude (Khait and Voskov, 2017).

In this paper, we extend the OBL method to a general purpose thermal-compositional reservoir simulation. ADGPRS is used as an implementation framework and as the reference approach for fidelity and performance comparisons. We apply the extended OBL to the several reservoir simulation problems of practical interest. Better nonlinear performance with the coarser representation of physics is demonstrated, while the approximation error is controlled by the resolution of the interpolation tables. Several advantages and extensions of the proposed method are discussed in the conclusion.

2. Conventional modeling approach

In this section, we describe one of the conventional nonlinear formulations for a general purpose thermal-compositional model. This formulation was implemented in ADGPRS (Voskov and Tchelepi, 2012) and is used in this paper as the reference solution.

2.1. Governing equations

Here, we describe the flow of energy and mass in a system with n_p phases and n_c components. For this model, n_c component mass conservation equations and a single energy conservation equation need to be written as

$$\frac{\partial}{\partial t}\left(\phi \sum_{p=1}^{n_p} x_{cp}\rho_p s_p\right) + \mathrm{div}\sum_{p=1}^{n_p} x_{cp}\rho_p \vec{u}_p + \sum_{p=1}^{n_p} x_{cp}\rho_p \tilde{q}_p = 0, \quad c = 1, \ldots, n_c, \tag{1}$$

$$\frac{\partial}{\partial t}\left(\phi \sum_{p=1}^{n_p} \rho_p s_p U_p + (1-\phi)U_r\right) + \mathrm{div}\sum_{p=1}^{n_p} h_p\rho_p \vec{u}_p + \mathrm{div}(\kappa\nabla T) + \sum_{p=1}^{n_p} h_p\rho_p \tilde{q}_p = 0. \tag{2}$$

All terms of the system (1)–(2) can be characterized as functions of the spatial coordinates $\boldsymbol{\xi}$ and physical state $\boldsymbol{\omega}$ as follows:

- $\phi(\boldsymbol{\xi}, \boldsymbol{\omega})$ – effective rock porosity,
- $x_{cp}(\boldsymbol{\omega})$ – component concentration in phase,
- $\rho_p(\boldsymbol{\omega})$ – phase molar density,
- $s_p(\boldsymbol{\omega})$ – phase saturation,
- $\vec{u}_p(\boldsymbol{\xi}, \boldsymbol{\omega})$ – phase velocity,
- $\tilde{q}_p(\boldsymbol{\xi}, \boldsymbol{\omega}, \mathbf{u})$ – source of phase,
- $\mathbf{U}_p(\boldsymbol{\omega})$ – phase internal energy,
- $\mathbf{U}_r(\boldsymbol{\xi}, \boldsymbol{\omega})$ – rock internal energy,
- $h_p(\boldsymbol{\omega})$ – phase enthalpy,
- $\kappa(\boldsymbol{\xi}, \boldsymbol{\omega})$ – thermal conduction.

The only exception here is the phase source term which also depends on $\mathbf{u}$ – well control variables.

Next, for simplicity, we assume that the rock internal energy and thermal conduction are spatially homogeneous, thus

$$U_r = f(\boldsymbol{\omega}), \quad \kappa = f(\boldsymbol{\omega}). \tag{3}$$

Phase flow velocity is assumed to follow the Darcy law as

$$\vec{u}_p = -\left(\mathbf{K}\frac{k_{rp}}{\mu_p}\left(\nabla p_p - \vec{\gamma}_p \nabla D\right)\right), \tag{4}$$

where

- $\mathbf{K}(\boldsymbol{\xi})$ – effective permeability tensor,
- $k_{rp}(\boldsymbol{\omega})$ – phase relative permeability,
- $\mu_p(\boldsymbol{\omega})$ – phase viscosity,
- $p_p(\boldsymbol{\omega})$ – phase pressure,
- $\vec{\gamma}_p(\boldsymbol{\omega})$ – gravity vector,
- $D(\boldsymbol{\xi})$ – depth (backward oriented).

After application of a finite-volume discretization on a general unstructured mesh and backward Euler approximation in time, we get

$$V\left(\left(\phi\sum_{p=1}^{n_p} x_{cp}\rho_p s_p\right)^{n+1} - \left(\phi\sum_{p=1}^{n_p} x_{cp}\rho_p s_p\right)^{n}\right) - \Delta t\sum_{l}\left(\sum_{p=1}^{n_p} x_{cp}^{l}\rho_p^{l}\Gamma_p^{l}\Delta\psi^{l} + \Delta t\sum_{p=1}^{n_p} x_{cp}\rho_p \mathbf{q}_p = 0\right), \tag{5}$$

$$V\left[\left(\phi\sum_{p=1}^{n_p}\rho_p s_p U_p + (1-\phi)U_r\right)^{n+1} - \left(\phi\sum_{p=1}^{n_p}\rho_p s_p U_p + (1-\phi)U_r\right)^{n}\right] - \Delta t\sum_{l}\left(\sum_{p=1}^{n_p} h_p^{l}\rho_p^{l}\Gamma_p^{l}\Delta\psi^{l} + \Gamma_c^{l}\Delta T^{l}\right) + \Delta t\sum_{p=1}^{n_p} h_p\rho_p\mathbf{q}_p = 0, \tag{6}$$

where V is the control volume of a grid cell and $q_p = \tilde{q}_p V$ is the source of a phase p. Here, we have neglected capillarity, gravity and used Two-Point Flux Approximation (TPFA) with upstream weighting. Therefore, $\Delta\psi^{l}$

becomes the simple difference in pressures over an interface l, and similarly ΔT^l is the temperature difference between the neighboring blocks. In addition, $\Gamma_p^l = \Gamma^l k_{rp}^l / \mu_p^l$ is a phase transmissibility, with Γ^l assumed to be the constant geometrical part of transmissibility, including permeability and the geometry of the control volume. For the energy conservation equation, an additional term Γ_c^l corresponds to conductive transmissibility, which includes a thermal conduction of all phases (including solid) and the geometry as

$$\Gamma_c^l = \Gamma^l \left(\phi \left(\sum_{p=1}^{n_p} s_p \kappa_p \right) + (1-\phi)\kappa_r \right). \tag{7}$$

2.2. Nonlinear formulation and linearization

Equations (5) and (6) are approximated in time using the Fully Implicit Method (FIM). The method suggests that the convective flux terms from mass and energy conservation equations, as well as the energy conductive flux, depend on the values of nonlinear unknowns at the current time step. This introduces nonlinearity into the system, which is further increased by the closure assumption of instantaneous thermodynamic equilibrium. Here, we apply the thermal extension of the overall molar formulation (Collins et al., 1992) for nonlinear solution of the governing equations. An exact thermodynamic equilibrium is required at every nonlinear iteration in this formulation. Hence, for any grid block that contains a multiphase (n_p) multicomponent (n_c) mixture, we solve the following system:

$$F_c = z_c - \sum_{p=1}^{n_p} \nu_p x_{cp} = 0, \tag{8}$$

$$F_{c+n_c} = f_{c1}(p, T, \mathbf{x}_1) - f_{cp}(p, T, \mathbf{x}_p) = 0, \tag{9}$$

$$F_{p+n_c \times n_p} = \sum_{c=1}^{n_c} (x_{c1} - x_{cp}) = 0, \tag{10}$$

$$F_{n_p+n_c \times n_p} = \sum_{p=1}^{n_p} \nu_p - 1 = 0, \tag{11}$$

In this procedure, which is usually called multiphase flash (Michelsen, 1982), $z_c = \sum_p x_{cp}\rho_p s_p / \sum_p \rho_p s_p$ is the overall composition, and $f_{cp}(p, T, x_{cp})$ is the fugacity of a component c in a phase p. By solving this system, we obtain mole fractions for each component x_{cp} and phase fractions ν_p for the given overall composition z_c. In the molar formulation, the nonlinear unknowns are p, z_c, and T (or h), therefore the physical state $\boldsymbol{\omega}$ is completely defined by these variables.

After obtaining the solution of multiphase flash, we determine partial derivatives with respect to nonlinear unknowns using the inverse theorem (see Voskov and Tchelepi, 2012 for details) and assemble the Jacobian and residuals. This step is often called linearization. The conventional linearization approach is based on the Newton-Raphson method, which solves on each nonlinear iteration the following linear system of equations:

$$\mathbf{J}(\boldsymbol{\omega}^k)(\boldsymbol{\omega}^{k+1} - \boldsymbol{\omega}^k) + \mathbf{r}(\boldsymbol{\omega}^k) = 0, \tag{12}$$

where $J(\boldsymbol{\omega}_k)$ and $r(\boldsymbol{\omega}_k)$ are the Jacobian and residual defined at a nonlinear iteration k. The conventional approach assumes the numerical representation of rock and fluid properties and their derivatives with respect to nonlinear unknowns. This may require either table interpolation (e.g., for relative permeability) or the solution of a highly nonlinear system (8)–(11) for properties defined by an Equation of State (EoS) in combination with the chain rule and inverse theorem. As a result, a nonlinear solver has to resolve all of the small features of the property descriptions, which can be quite challenging and is often unnecessary due to the numerical nature and uncertainties in property evaluation.

3. Proposed modeling approach

In this section, we describe the thermal multicomponent extension of the approach developed by Voskov (2017) for isothermal systems.

3.1. Computation of partial derivatives during multilinear interpolation

The key advantage of the proposed approach is the extensive usage of piecewise multilinear generalization of piecewise bilinear interpolation for an N-dimensional space at the linearization stage. We chose this approach for its application simplicity in comparison with the approach proposed in Zaydullin et al. (2013) for compositional systems with a large number of components. Both methods have comparable accuracy and performance when applied to systems with a limited number of degrees of freedom, see Weiser and Zarantonello (1988) for details.

An interpolant approximation $A(x_1, \ldots, x_N)$ to a function $\alpha(x_1, \ldots, x_N)$ can be built using interpolation table values of α:

$$\{\alpha(X_{i_1}, X_{i_2}, \ldots, X_{i_N}) : i_1 = 1, \ldots, n_1, \ldots, i_N = 1, \ldots, n_N\}, \tag{13}$$

where $n_1, \ldots, n_N$ are the numbers of points along interpolation axes. The first step of the method is to find table intervals (X_{I_1}, X_{I_1+1}), $\ldots, (X_{I_N}, X_{I_N+1})$ such that

$$X_{I_1} \le x_1 \le X_{I_1+1}, \ldots, X_{I_N} \le x_N \le X_{I_N+1}. \tag{14}$$

In order to further simplify description, we scale each of the intervals to $(0, 1)$. That allows us to reformulate the problem to finding an approximation $\Pi(y_1, \ldots, y_N)$ for a function $\pi(y_1, \ldots, y_N)$ defined over the unit N-cube, described as

$$0 \le y_1 \le 1, \ldots, 0 \le y_N \le 1, \tag{15}$$

where

$$y_i = \frac{x_i - X_{I_i}}{X_{I_i+1} - X_{I_i}}, \tag{16}$$

using the table values

$$\{\pi(j_1, \ldots, j_N) = \alpha(X_{i_1+j_1}, , \ldots, X_{i_N+j_N}) : j_1 = 0 \text{ or } 1, \ldots, j_N = 0 \text{ or } 1\}. \tag{17}$$

The piecewise multilinear approximation is computed in a recursive manner. First, we define

$$\Pi_1^i = \Pi(j_1, \ldots, j_{i-1}, 1, y_{i+1}, \ldots, y_N), \tag{18}$$

$$\Pi_0^i = \Pi(j_1, \ldots, j_{i-1}, 0, y_{i+1}, \ldots, y_N).$$

Then,

$$A = \Pi(y_1, \ldots, y_N), \tag{19}$$

$$\Pi(j_1, \ldots, j_i, y_{i+1}, \ldots, y_N) = \Pi_0^i + y_i(\Pi_1^i - \Pi_0^i), \quad i = 1, \ldots, N, \tag{20}$$

where the table values are

$$\Pi(j_1, \ldots, j_N) = \pi(j_1, \ldots, j_N). \tag{21}$$

The partial derivatives are determined in a similar way. First,

$$\begin{aligned} \Pi_1^{ki} &= \Pi^k(j_1, \ldots, j_{i-1}, 1, y_{i+1}, \ldots, y_N), \\ \Pi_0^{ki} &= \Pi^k(j_1, \ldots, j_{i-1}, 0, y_{i+1}, \ldots, y_N), \end{aligned} \tag{22}$$

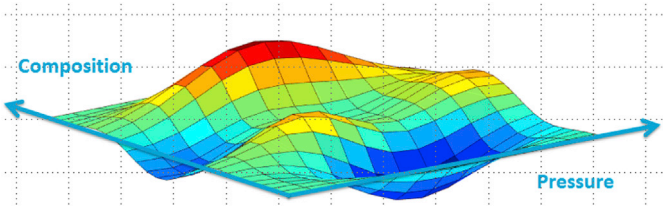

Fig. 1. 2D parametrization of an abstract operator.

and then

$$\frac{\delta\alpha}{\delta x_k} = \frac{\delta A}{\delta x_k} = \Pi^k(y_1, \ldots, y_N), \tag{23}$$

$$\Pi^k(j_1, \ldots, j_i, y_{i+1}, \ldots, y_N) = \begin{cases} \Pi_0^{ki} + y_i\left(\Pi_1^{ki} - \Pi_0^{ki}\right), & i = 1, \ldots, k, \\ \dfrac{\Pi_1^i - \Pi_o^i}{X_{l_i+1} - X_{l_i}}, & i = k, \\ \Pi_0^i + y_i\left(\Pi_1^i - \Pi_0^i\right), & i = k+1, \ldots, N. \end{cases} \tag{24}$$

3.2. Operator form of the conservation equations

In order to apply the described approximation method, we rewrite equations (5) and (6), representing each term as a product of state-dependent and space-dependent operators (Voskov, 2017). In addition, we assume the porosity as a pseudo-physical state variable ($\phi \in \boldsymbol{\omega}$).

The resulting mass conservation equation is

$$a(\boldsymbol{\xi})(\alpha_c(\boldsymbol{\omega}) - \alpha_c(\boldsymbol{\omega}_n)) + \sum_l b(\boldsymbol{\xi}, \boldsymbol{\omega})\beta_c(\boldsymbol{\omega}) + \theta_c(\boldsymbol{\xi}, \boldsymbol{\omega}, \mathbf{u}) = 0, \quad c = 1, \ldots, n_c. \tag{25}$$

Here

$$a(\boldsymbol{\xi}) = \phi V(\boldsymbol{\xi}), \tag{26}$$

$$\alpha_c(\boldsymbol{\omega}) = \sum_{p=1}^{n_p} x_{cp}\rho_p s_p, \tag{27}$$

$$b(\boldsymbol{\xi}, \boldsymbol{\omega}) = \Delta t \Gamma^l(\boldsymbol{\xi})\left(p^b - p^a\right), \tag{28}$$

$$\beta_c(\boldsymbol{\omega}) = \sum_{p=1}^{n_p} x_{cp}^l \rho_p^l \frac{k_{rp}^l}{\mu_p^l}, \tag{29}$$

$$\theta_m(\boldsymbol{\xi}, \boldsymbol{\omega}, \mathbf{u}) = \Delta t \sum_{p=1}^{n_p} x_{cp}\rho_p q_p(\boldsymbol{\xi}, \boldsymbol{\omega}, \mathbf{u}). \tag{30}$$

In the equations above, c_r is a rock compressibility, while $\boldsymbol{\omega}$ and $\boldsymbol{\omega}_n$ are nonlinear unknowns on the current and the previous time step respectively.

The modified energy conservation equation becomes

$$a_e(\boldsymbol{\xi})(\alpha_e(\boldsymbol{\omega}) - \alpha_e(\boldsymbol{\omega}_n)) + \sum_l b_e(\boldsymbol{\xi}, \boldsymbol{\omega})\beta_e(\boldsymbol{\omega}) + \sum_i c_e(\boldsymbol{\xi}, \boldsymbol{\omega})\gamma_e(\boldsymbol{\omega}) + \theta_e(\boldsymbol{\xi}, \boldsymbol{\omega}, \mathbf{u}) = 0, \tag{31}$$

where

$$a_e(\boldsymbol{\xi}) = V(\boldsymbol{\xi}), \tag{32}$$

$$\alpha_e(\boldsymbol{\omega},) = \phi\left(\sum_{p=1}^{n_p} \rho_p s_p U_p - U_r\right) + U_r, \tag{33}$$

$$b_e(\boldsymbol{\xi}, \boldsymbol{\omega}) = b_m(\boldsymbol{\xi}, \boldsymbol{\omega}), \tag{34}$$

$$\beta_e(\boldsymbol{\omega}) = \sum_{p=1}^{n_p} h_p^l \rho_p^l \frac{k_{rp}^l}{\mu_p^l}, \tag{35}$$

$$c_e(\boldsymbol{\xi}) = \Delta t \Gamma^l\left(T^b - T^a\right), \tag{36}$$

$$\gamma_e(\boldsymbol{\omega}) = \phi\left(\sum_{p=1}^{n_p} s_p \kappa_p - \kappa_r\right) + \kappa_r, \tag{37}$$

$$\theta_e(\boldsymbol{\xi}, \boldsymbol{\omega}, \mathbf{u}) = \Delta t \sum_{p=1}^{n_p} h_p \rho_p q_p(\boldsymbol{\xi}, \boldsymbol{\omega}, \mathbf{u}). \tag{38}$$

In these derivations, T^a and T^b are assumed to be the temperatures in neighboring grid blocks a and b.

This representation allows us to identify and distinguish the physical state dependent operators - $\alpha_c, \beta_c, \alpha_e, \beta_e, \gamma_e$ in both mass (5) and energy (6) conservation equations. The source/sink term can also be processed in a similar manner, but we have left this out of this work and perform a conventional treatment for this operator.

3.3. Operator-based linearization approach

The proposed approach simplifies the description of fluid and rock properties by building approximation interpolants for the operators $\alpha_c, \beta_c, \alpha_e, \beta_e, \gamma_e$ within the parameter space of a simulation problem. For a general non-isothermal compositional problem with n_c components, the method requires $[2n_c + 3]$ operators. If fluid properties change spatially and several PVT and SCAL regions are employed, several sets of operators need to be introduced accordingly. The values of the operators are fully determined by the set of $N = [n_c + 1]$ independent variables $\{p, T, z_1, \ldots, z_{n_c-1}\}$. The pressure and temperature ranges in the compositional parameter space can usually be determined by conditions specified for wells, while the overall composition is naturally bounded by the interval [0,1]. As mentioned above, we add the porosity as a pseudo-physical state variable with the corresponding range.

Next, we parametrize the interval of each state variable using, for simplicity, the same number $n = n_1 = \ldots = n_N$ of uniformly distributed points on the intervals of parameters, according to (13). This results in the set of vectors $(p_i, T_i, z_{1_i} \ldots, z_{n_c-1_i}, \phi_i) : i = 1, \ldots, n$, which can be interpreted as the discrete representation of the physical space in a simulation. At the pre-processing stage, or adaptively, we can evaluate the operators $\alpha_c, \beta_c, \alpha_e, \beta_e, \gamma_e$ at every point in the discrete parameter space and store them in $(n_c + 2)$ -dimensional tables A_e and Γ_e and $(n_c + 1)$ -dimensional tables A_c, B_c, B_e. Fig. 1 illustrates an example for an abstract operator, parametrized in two-dimensional space. During the simulation, we interpolate both the values and the partial derivatives of all state-dependent operators, using tables created for each grid block. This provides a continuous description based on the interpolation operator, whose accuracy is controlled by the resolution of discretization in parameter space. For an isothermal compositional problem, we preserve only mass conservation operators α_c, β_c, defined by $\{p, z_1, \ldots, z_{n_c-1}\}$.

This representation significantly simplifies the implementation of complex simulation frameworks. Instead of keeping track of each property and its derivatives with respect to nonlinear unknowns, we can construct an algebraic system of equations with abstract algebraic operators representing the complex physics. The performance of this formulation benefits from the fact that all expensive evaluations can be performed using a limited number of supporting points. Finally, the

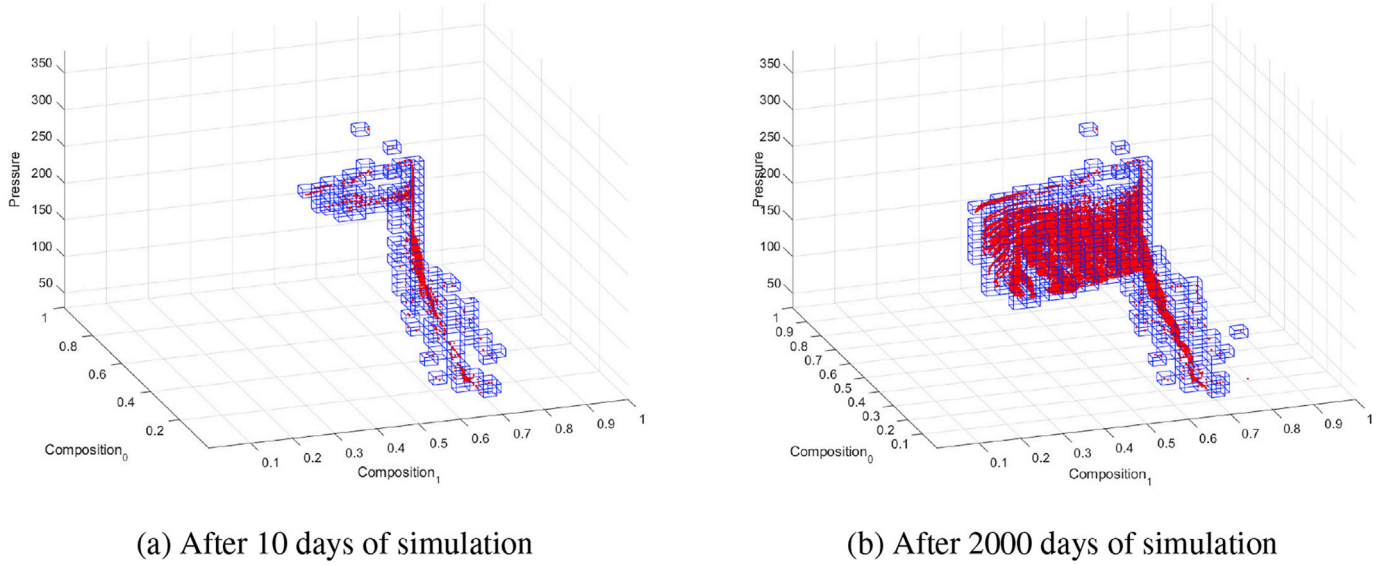

Fig. 2. Adaptive operator-based linearization approach.

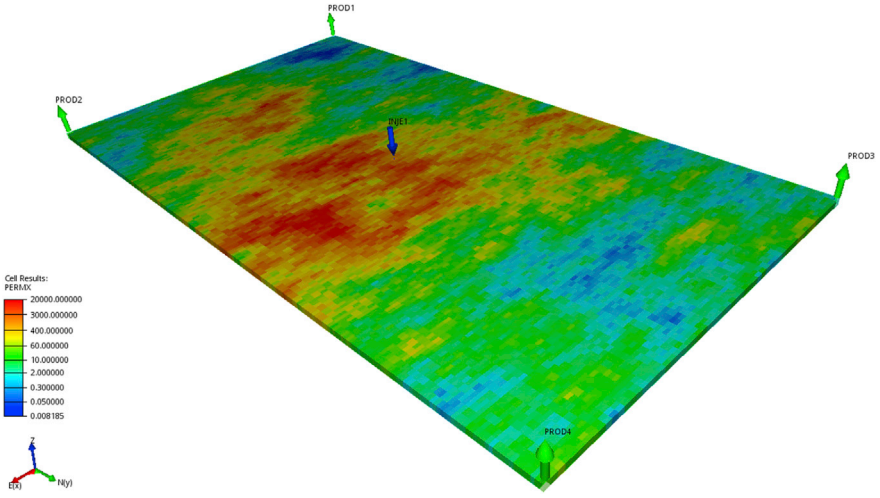

Fig. 3. Reservoir permeability map used for all simulations.

performance of the nonlinear solver can be improved since the Jacobian is constructed based on a combination of piece-wise linear operators directly dependent on the nonlinear unknowns.

3.4. Adaptive operator-based linearization

The total size of the interpolation tables is defined by the number of dimensions N and the number of interpolation points n as n^N. While the dimensionality depends on the number of components and thermal assumptions in a problem of interest, the number of interpolation points corresponds to the desired accuracy of the physical representation. Therefore, parametrization at the pre-processing stage would require substantial amount of memory for multicomponent systems modeled at high interpolation precision. Furthermore, the necessity of searching base points (i.e., operator values) for every interpolation in a huge array of data affects the performance of the simulation. Notice that due to the hyperbolic nature of some variables (e.g., overall compositions), the vast majority of parameter space remains unused (Iranshahr et al., 2013; Zaydullin et al., 2013).

The adaptive approach avoids these disadvantages by removing the need for the entire pre-processing stage (Zaydullin et al., 2013). In this approach, base points are computed only when they are required by the current physical state of a control volume. The obtained operator values are then employed in the interpolation process and stored for future use. Consequently, the method adds a new base point and computes appropriate operators, if the base point was not computed before. In the end of the simulation, the resulting sparse multi-dimensional table of stored operators represents an actual subspace of physical parameters used in the process. For example, Fig. 2 shows an adaptive parametrization in the parameter space for a black oil simulation at two different time steps. The adaptive approach reproduces exact numerical results of the pre-processing method used in Voskov (2017) with greatly improved overall performance, especially for multicomponent systems.

4. Numerical results

In this section, we present numerical results for flow and transport simulations, which employed the adaptive operator-based linearization for different physics. A convergence study and an error analysis are provided for different resolutions of the physical parameter space, using simulation results for the conventional linearization approach as the reference solution. In addition, we present the comparison of simulation

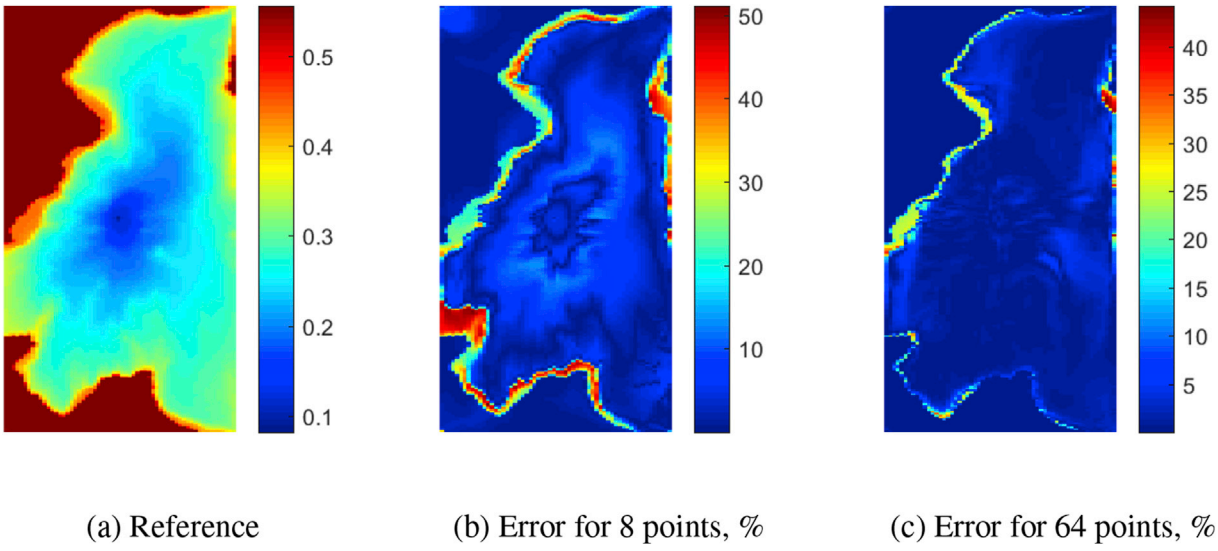

Fig. 4. Oil composition solution at t = 8000 days.

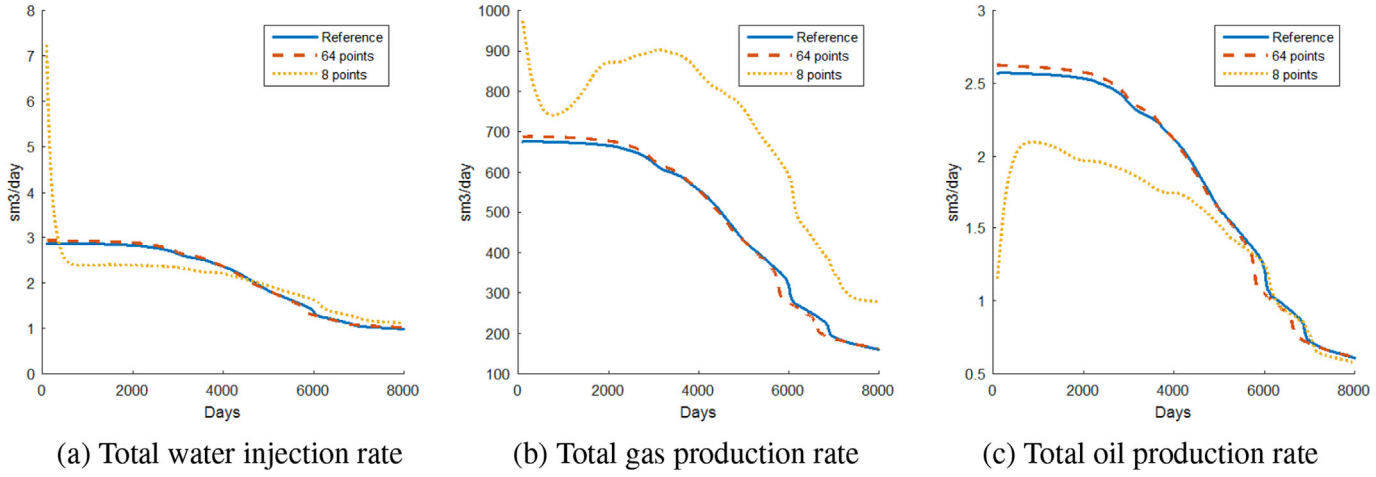

Fig. 5. Total well rates for reference solution, OBL with 8 points, and OBL with 64 points.

time for a single forward run of each type of physics. The improvement in the performance of OBL-based simulations is achieved by a lower number of nonlinear iterations (which is almost directly proportional to the runtime) and the absence of iterative phase behavior computations in OBL method.

To demonstrate the general purpose applicability of the proposed approach, we conduct our study using black-oil, compositional, and thermal-compositional physical kernels often used in reservoir simulation. All problems are modeled within the same highly-heterogeneous reservoir shown in Fig. 3. It represents the 7-th layer of the SPE10 model (Christie and Blunt, 2001) consisting of 60×220 grid cells, where the size of every grid cell is $6 \times 3 \times 0.6$ meters. The porosity of the reservoir was defined constantly as $\phi = 0.4$. An injection well is placed in the middle of the reservoir, with four producers set at the corners.

Table 1
Results of black oil simulation.

Resolution	Iters.	E_p, %	E_{z_g}, %	E_{z_o}, %	E_{z_w}, %	Space,%	CPU, sec.
Std.	6162	–	–	–	–	–	1090
64	3284	0.15	1.95	2.03	2.03	0.789	518
32	3067	0.27	2.21	2.12	2.15	1.965	495
16	3332	0.47	11.26	3.43	4.54	6.238	545
8	2787	0.99	30.01	6.60	10.47	17.188	466

4.1. Black-oil physics kernel

Here, we used a standard black-oil formulation, where only a gas component can dissolve in oil phase and the most of the properties described as a table-based correlations. The water injection well operated with Bottom Hole Pressure (BHP) control at a pressure $P_i = 350$ bar, and the producer well operated at $P_p = 250$ bar. The reservoir was initialized uniformly with pressure $P_0 = 300$ bar, water saturation $S_w = 0.2$, gas saturation $S_g = 0$ and bubble pressure $P_{bub} = 270$ bar. All simulations were run for 8000 days with a maximum timestep of $\Delta t = 10$ days.The PVT properties, relative permeabilities, and capillary pressure tables from SPE 9 test case (Killough, 1995) were used.

Fig. 4 represents a reference solution for oil composition at the last timestep and error maps for operator-based linearization with 8- and 64-points. The error maps were calculated as the absolute difference between a reference solution and a solution from the proposed approach, normalized by the amplitude of the reference solution. It is easy to see that the error reduces significantly with increasing number of points. Also, the error reaches its maximum along the displacement front. These conclusions are also valid for water and gas compositions in this model, and all the models described below. Total well rates comparison is shown in Fig. 5. While OBL with 8 point resolution provides completely different curve shapes, 64 points is enough to capture the wells behavior quite

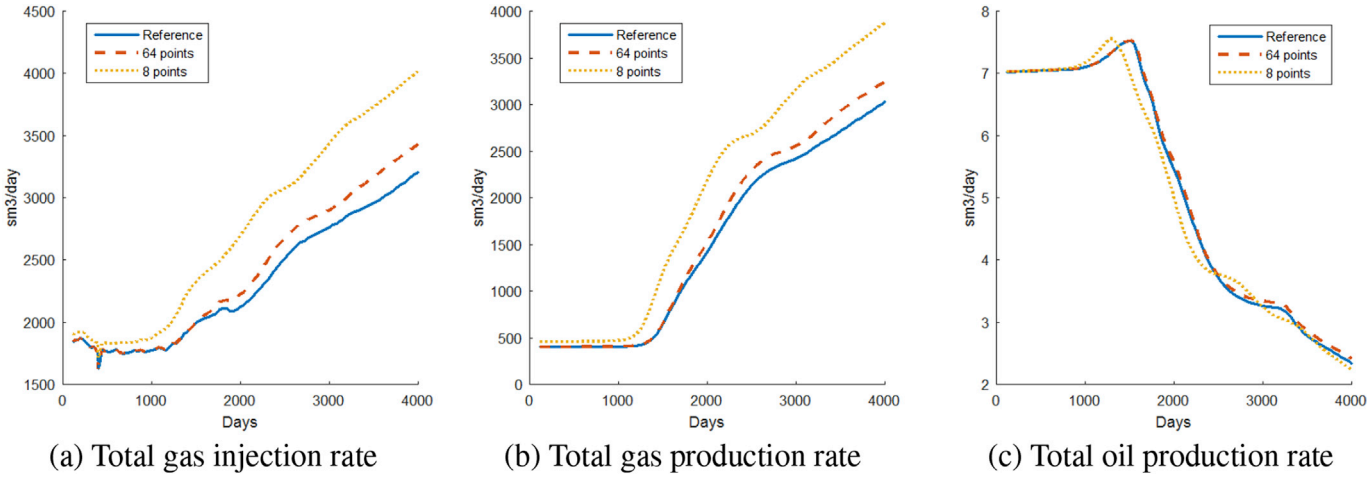

Fig. 6. Total well rates for reference solution, OBL with 8 points, and OBL with 64 points.

Table 2
Results of isothermal compositional simulation.

Resolution	Iters.	E_p, %	E_{CO_2}, %	E_{C_1}, %	E_{C_4}, %	$E_{C_{10}}$, %	Space,%	CPU, sec
Std.	710	–	–	–	–	–	–	616
64	629	0.29	0.65	1.02	0.64	0.76	0.133	170
32	583	0.30	0.95	1.56	0.90	1.17	0.471	142
16	569	0.32	1.78	2.70	1.87	2.17	1.784	137
8	587	0.72	3.62	5.51	5.29	4.52	8.801	140

accurately.

To perform a convergence analysis for the new linearization method, the following relation for the error was introduced:

$$E = \frac{1}{n}\sum_{i=1}^{n}\frac{\left|x_{obl}^{i} - x_{ref}^{i}\right|}{\left(\max\left(\mathbf{x}_{ref}\right) - \min\left(\mathbf{x}_{ref}\right)\right)}, \tag{39}$$

where:

- n – number of grid blocks in the model,
- x_{obl}^{i} – the solution based on operator-based linearization,
- x_{ref}^{i} – the reference solution.

This error was estimated for every state variable at the end of the simulation. Overall results are shown in Table 1. The resolution of physical space, defined by the number of interpolation points, is in the first column. The total number of nonlinear iterations is shown in the second column. The next three columns show an estimation error in pressure, composition of gas, water, and oil, respectively. The next column shows the percent of points used for adaptive parametrization of physical space by the operator-based linearization approach. And finally, the last column reflects a CPU time required for a serial run on Intel Xeon E5-1620 @ 3.5 GHz.

Table 1 demonstrates that a smaller number of interpolation points results in more linear physics, leading to a smaller number of Newton iterations. The only exception is the 16 points resolution where the number of nonlinear iterations is higher than that for the other resolutions. This reflects the fact that the location of points in current approach was blindly based on a uniform distribution. However, even for this case, the number of Newton iterations is significantly less than that for the standard simulation. Hence, the corresponding time is also reduced significantly.

4.2. Isothermal compositional kernel

Next, we demonstrate an applicability of OBL technique for the

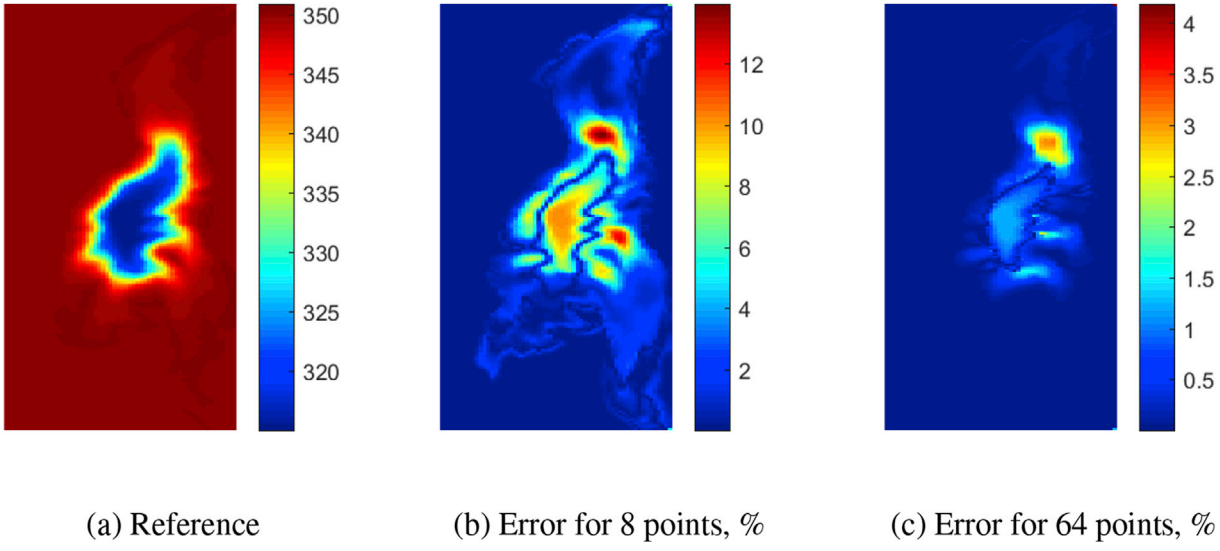

Fig. 7. Temperature solution at t = 2000 days.

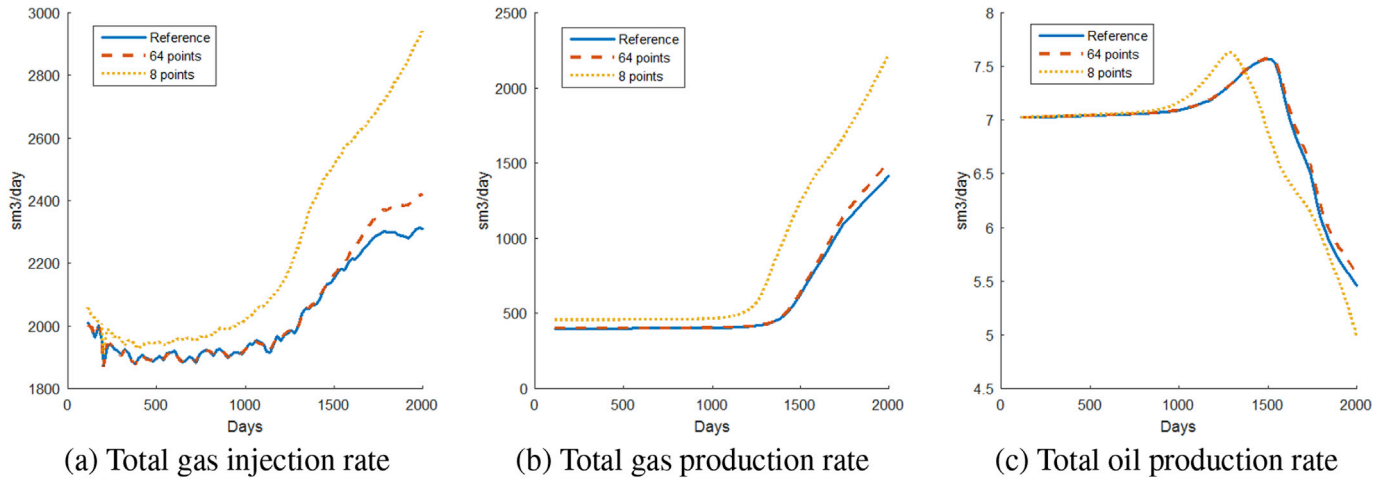

Fig. 8. Total well rates for reference solution, OBL with 8 points, and OBL with 64 points.

Table 3
Results of non-isothermal compositional simulation.

Resolution	Iters.	E_p, %	E_T, %	E_{CO_2}, %	E_{C_1}, %	E_{C_4}, %	$E_{C_{10}}$, %	Space,%	CPU, sec
Std.	647	–	–	–	–	–	–	–	628
64	587	0.12	0.12	0.19	0.37	0.20	0.21	0.005	317
32	553	0.12	0.27	0.33	0.67	0.35	0.37	0.037	234
16	536	0.14	0.48	1.15	2.02	1.21	1.35	0.241	209
8	555	0.41	1.21	2.79	5.16	3.64	3.86	2.371	217

isothermal process of carbon dioxide and methane injection into oil with composition from Orr et al. (1995). The initial oil was made of 4 components CO_2, C_1, C_4, and C_{10} at corresponding compositions: 1% of carbon dioxide, 11% of methane, 38% of n-butane, and 50% of decane. We injected a mixture of 80% of CO_2 and 20% of CH_4 at a BHP $P_i = 120$ bar. The production wells operated at BHP $P_p = 60$ bar. The initial pressure was $P_0 = 90$ bars and temperature $T_0 = 350$ K. The simulation period was 4000 days with a maximum time step $\Delta t = 40$ days. The description of phase behavior and properties based on Peng-Robinson Equation of State (Peng and Robinson, 1976) was used in this kernel.

In this case, as shown on Fig. 6, OBL with 8 point resolution significantly overestimates gas injection and production, while finer OBL resolution matches the reference solution exactly during first 2000 days and deviates with small margin later. Oil production is captured well even by coarser OBL, while the finer parametrization provides almost complete match. Table 2 shows the main results of the isothermal simulation. The difference in the number of Newton iterations number between the standard and operator-based linearization simulations is significantly less than in the previous case, but the trend is similar with an exception now for 8 points. The performance of simulation with OBL approach was improved even more significantly in comparison to conventional simulation. It can be explained by an expensive phase behavior evaluations performed for compositional kernel in comparison to black oil kernel. They are only required in conventional simulation and almost completely absent in the OBL approach.

4.3. Thermal-compositional kernel

The next simulation model was built on a thermal-compositional physical kernel. The initial and injection conditions stayed the same as in the previous example except that the injection mixture had a lower temperature of $T = 315$ K. The simulation period was 2000 days with a maximum time step of $\Delta t = 20$ days. Temperature distribution at the last time step and corresponding errors are depicted in Fig. 7. The errors are concentrated near the cooling front (similar with composition errors located near the displacement front) and the injection well. The latter can be explained by a larger nonlinearity in the energy conservation equation, introduced by a correlation for enthalpy.

It can be seen from Fig. 8 that OBL with 64 points resolution again demonstrates the precise capturing of injection and production rates by for the first 1500 days of simulation with small deviations during the last 500 days. The convergence results of the thermal-compositional simulation are presented in Table 3 and is similar to the isothermal model. In this simulation, the region of adaptive parametrization of physical space drops down to 0.001% which reflects the importance of the adaptive approach for higher dimensional systems (system with more nonlinear unknowns).

5. Conclusions

In this work, we presented a new approach for linearization of the general purpose reservoir simulation problem. In operator-based linearization method, the governing equations are represented in an operator form where each term is the product of two operators: the first is fully defined by the physical state of a problem, and the second depends on both spatial and state variables. We introduced parametrization of the first type of operators using a uniformly distributed mesh in parameter space of physical problem. The second type of operators was treated in conventional manner. An adaptive parametrization in the physical space was applied to reduce the memory consumption and increase the efficiency of the interpolation procedure.

We demonstrated the applicability of the new linearization approach for reservoir simulation with different physical kernels. In particular, black-oil, isothermal, and non-isothermal compositional kernels were tested in a highly heterogeneous reservoir. We showed that the proposed operator-based linearization approach reproduces the results of the reference solution on a fine parametrization grid. At the same time, the coarsening of parameter space improves the nonlinear solution and resulting performance of simulation while errors in physical approximations remain under control.

The main benefits of the proposed approach are: the simplicity of an

application, potential improvements in the nonlinear convergence, and a generic approach to coarsening the physics in general purpose reservoir simulation. The application of a trust region technique, similar to (Voskov and Tchelepi, 2011), looks like the best candidate for the improvement of nonlinear convergence in complex simulations. Future work will include the developing of advanced nonlinear solvers as well as balancing errors in spatial, temporal, and physical approximation to achieve better performance and accuracy of reservoir simulations.

Acknowledgments

We acknowledge the Stanford University Petroleum Research Institute for Reservoir Simulation (SUPRI-B) program for the financial support and permission to use ADGPRS in this research.

References

Aziz, K., Settari, T., 1979. Petroleum Reservoir Simulation. Applied Science Publishers.
Cao, H., 2002. Development of Techniques for General Purpose Simulators. PhD Thesis. Stanford University.
Cao, H., Crumpton, P., Schrader, M., 2009. Efficient General Formulation Approach for Modeling Complex Physics, vol. 2, pp. 1075–1086.
Christie, M., Blunt, M., 2001. Tenth SPE comparative solution project: a comparison of upscaling techniques. SPE Reserv. Eval. Eng. 4 (4), 308–316.
Collins, D., Nghiem, L., Li, Y.K., Grabenstetter, J., 1992. Efficient approach to adaptive-implicit compositional simulation with an equation of state. SPEJ 7 (2), 259–264.
Iranshahr, A., Voskov, D., Tchelepi, H., 2013. Tie-simplex based compositional space parameterization: continuity and generalization to multiphase systems. AIChE J. 59 (5), 1684–1701.
Khait, M., Voskov, D., 2017. GPU-offloaded general purpose simulator for multiphase flow in porous media. In: SPE Reservoir Simulation Conference. Society of Petroleum Engineers.
Killough, J.E., 1995. Ninth SPE comparative solution project: a reexamination of black-oil simulation. In: SPE Reservoir Simulation Symposium.
Krogstad, S., Lie, K.A., Moyner, O., Nilsen, H., Raynaud, X., Skaflestad, B., 2015. MRST-AD - an Open-source Framework for Rapid Prototyping and Evaluation of Reservoir Simulation Problems, vol. 3, pp. 2080–2105.
Michelsen, M., 1982. The Isothermal Flash Problem: Part II. Phase-split Calculation, vol. 9, pp. 21–40.
Muller, F., Jenny, P., Meyer, D., 2016. Parallel multilevel monte carlo for two-phase flow and transport in random heterogeneous porous media with sampling-error and discretization-error balancing. SPE J. 21 (6), 2027–2037.
Orr Jr., F., Dindoruk, B., Johns, R., 1995. Theory of multicomponent gas/oil displacements. Industrial Eng. Chem. Res. 34 (8), 2661–2669.
Peng, D.Y., Robinson, D.B., 1976. New two-constant equation of state. Ind. Eng. Chem. Fundam. 15 (1), 59–64.
Schlumberger, 2007. ECLIPSE Technical Description. Tech. Rep. Schlumberger, Houston.
Vanden, K., Orkwis, P., 1996. Comparison of numerical and analytical Jacobians. AIAA J. 34 (6), 1125–1129.
Voskov, D., Tchelepi, H., 2011. Compositional Nonlinear Solver Based on Trust Regions of the Flux Function along Key Tie-lines, vol. 2, pp. 799–809.
Voskov, D., Tchelepi, H., 2012. Comparison of nonlinear formulations for two-phase multi-component EoS based simulation. J. Petroleum Sci. Eng. 82-83, 101–111.
Voskov, D.V., 2017. Operator-based linearization approach for modeling of multiphase multi-component flow in porous media. J. Comput. Phys. 337, 275–288.
Weiser, A., Zarantonello, S., 1988. A note on piecewise linear and multilinear table interpolation in many dimensions. Math. Comput. 50 (181), 189–196.
Xu, T., Spycher, N., Sonnenthal, E., Zhang, G., Zheng, L., Pruess, K., 2011. Tough react version 2.0: a simulator for subsurface reactive transport under non-isothermal multiphase flow conditions. Comput. Geosciences 37 (6), 763–774.
Younis, R., 2011. Modern Advances in Software and Solution Algorithms for Reservoir Simulation. PhD Thesis. Stanford University.
Zaydullin, R., Voskov, D., Tchelepi, H., 2013. Nonlinear formulation based on an equation-of-state free method for compositional flow simulation. SPE J. 18 (2), 264–273.
Zaydullin, R., Voskov, D., Tchelepi, H., 2016. Phase-state identification bypass method for three-phase thermal compositional simulation. Comput. Geosci. 20 (3), 461–474.
Zhou, Y., Tchelepi, H., Mallison, B., 2011. Automatic differentiation framework for compositional simulation on unstructured grids with multi-point discretization schemes. In: SPE Reservoir Simulation Symposium.